JACS
JOURNAL OF THE AMERICAN CHEMICAL SOCIETY
Article
pubs.acs.org/JACS

Non-Fullerene-Acceptor-Based Bulk-Heterojunction Organic Solar Cells with Efficiency over 7%

Dan Sun,[†,‡,⊥] Dong Meng,[†,‡,⊥] Yunhao Cai,[§,∥] Bingbing Fan,[§,∥] Yan Li,[†] Wei Jiang,[†] Lijun Huo,[*,§,∥] Yanming Sun,[*,§,∥] and Zhaohui Wang[*,†]

[†]Beijing National Laboratory for Molecular Science, Key Laboratory of Organic Solids, Institute of Chemistry, Chinese Academy of Sciences, Beijing 100190, P. R. China

[‡]University of Chinese Academy of Sciences, Beijing 100049, P. R. China

[§]Key Laboratory of Bio-Inspired Smart Interfacial Science and Technology of Ministry of Education, Beijing Key Laboratory of Bio-inspired Energy Materials and Devices, School of Chemistry and Environment, Beihang University, Beijing 100191, P. R. China

[∥]Heeger Beijing Research and Development Center, International Research Institute for Multidisciplinary Science, Beihang University, Beijing 100191, P. R. China

Supporting Information

ABSTRACT: A novel perylene bisimide (PBI) dimer-based acceptor material, SdiPBI-S, was developed. Conventional bulk-heterojunction (BHJ) solar cells based on SdiPBI-S and the wide-band-gap polymer PDBT-T1 show a high power conversion efficiency (PCE) of 7.16% with a high open-circuit voltage of 0.90 V, a high short-circuit current density of 11.98 mA/cm^2, and an impressive fill factor of 66.1%. Favorable phase separation and balanced carrier mobilites in the BHJ films account for the high photovoltaic performance. The results demonstrate that fine-tuning of PBI-based materials is a promising way to improve the PCEs of non-fullerene BHJ organic solar cells.

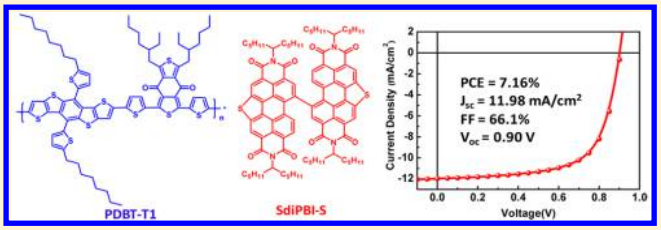

INTRODUCTION

Bulk-heterojunction (BHJ) organic solar cells comprising conjugated polymers and fullerene derivatives provide an effective solution for resolving the present energy crisis because of their low cost, light weight, and potential for roll-to-roll production as well as fabrication on flexible substrates.[1−8] In recent years, considerable effort has been devoted to exploring non-fullerene acceptors for use to replace fullerene derivatives in BHJ organic solar cells.[9−12] A number of high-performance non-fullerene acceptors have been recently developed and applied in BHJ organic solar cells with high power conversion efficiencies (PCEs) exceeding 6%.[13−16] Among the various classes of non-fullerene acceptors, perylene bisimide derivatives (PBIs) were some of the earliest and most common non-fullerene acceptors studied in BHJ organic solar cells because of their high electron mobility, strong absorption ability, and high environmental/thermal stability.[17−22] In spite of these favorable properties, PBI-based organic solar cells usually show low performance due to the formation of large aggregates in the active layer, where strong self-trapping of excitons occurs, severely limiting the exciton diffusion/separation process.[23−25] Accordingly, to avoid large crystalline aggregate domains, twisted PBI compounds have been designed,[14,15,26−39] mainly by means of PBI dimers linked at the imide positions or bay positions (the 1-, 6-, 7-, and 12-positions) either by direct attachment or through functional groups. Such kinds of PBI dimers yield BHJ organic solar cells with high PCEs over 6%.[14,15]

Fused and extended heteroarenes are recognized as very promising semiconducting materials because of a variety of intermolecular interactions induced by heteroatoms, such as van der Waals and heteroatom−heteroatom interactions, which are essential for achieving excellent device performance.[40−46] Moreover, incorporating heteroatoms into the carbon skeleton can alter the original structure as a result of the strain of five-membered heterorings. Heteroannulation in bay regions to construct bowl-shaped bis(perylene bismide)s has been reported previously.[47] In our previous work, we reported a bay-linked perylene bisimide acceptor, SdiPBI, which shows a high PCE of 5.9%.[30] In this study, SdiPBI was modified by insertion of two thiophene units in the bay positions, affording a new compound denoted as SdiPBI-S. The chemical structures of these two compounds are shown in Figure 1. Because of the electron-donating ability of the thiophene unit,, SdiPBI-S has a more twisted configuration and a higher lying LUMO energy in comparison with SdiPBI, which is favorable for improving the open-circuit voltage (V_{oc}) of solar cells.

In addition to extensive exploration of novel non-fullerene acceptors, the selection of appropriate electron donors to be paired with non-fullerene acceptors in BHJ systems plays a

Received: June 26, 2015
Published: August 17, 2015

DOI: 10.1021/jacs.5b06414
J. Am. Chem. Soc. 2015, 137, 11156−11162

Scheme 1. Synthesis of SdiPBI-S

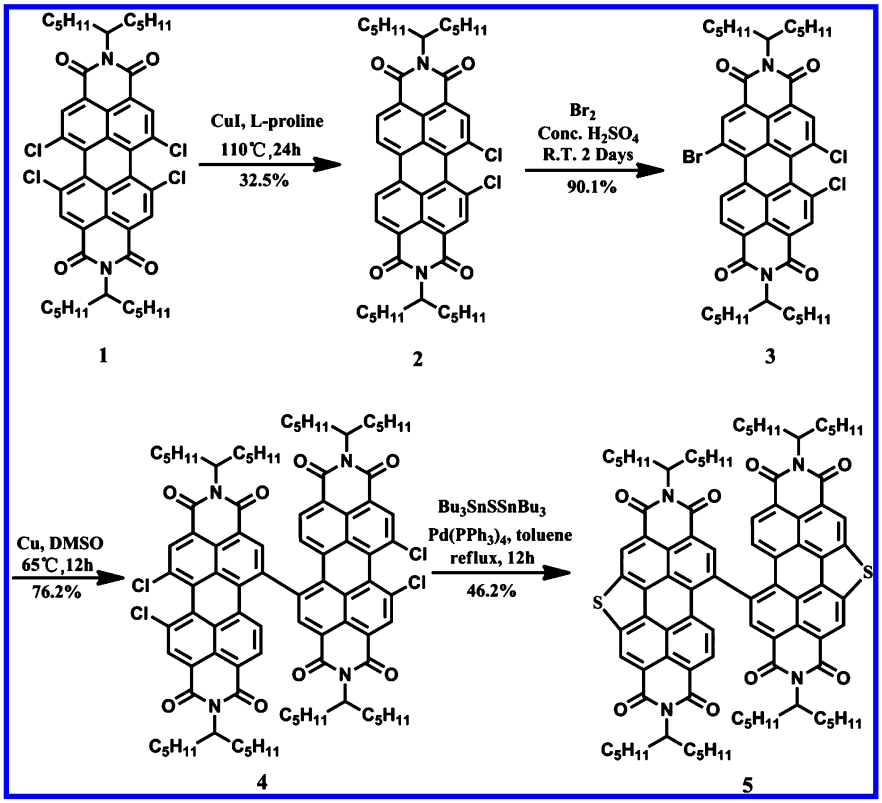

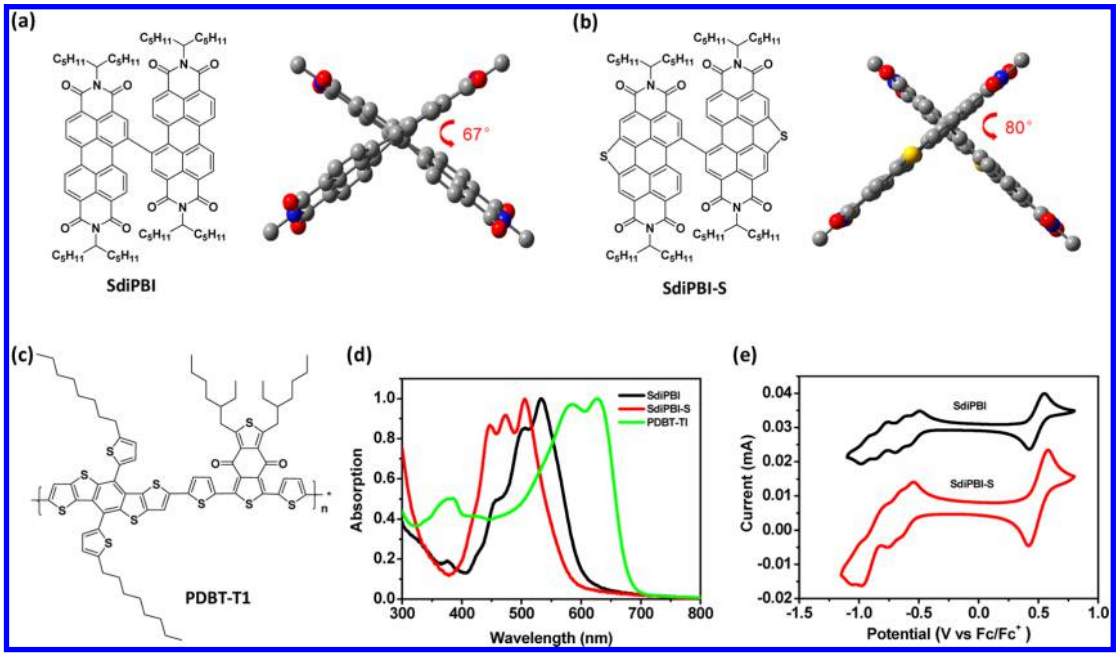

Figure 1. (a, b) Chemical structures of (a) SdiPBI and (b) SdiPBI-S and the corresponding side views of the optimized geometries obtained using DFT calculations at the B3LYP/6-31G(d) level. (c) Chemical structure of the donor PDBT-T1 used in this study. (d) Film absorption spectra of SdiPBI, SdiPBI-S, and PDBT-T1. (e) Cyclic voltammograms of SdiPBI and SdiPBI-S.

significant role in determining the morphology, open-circuit voltage, and photocurrent of organic solar cells. Here we report high-performance non-fullerene organic solar cells enabled by SdiPBI-S and a previously reported wide-band-gap polymer, PDBT-T1.[48] The excellent hole mobility, the complementary absorption spectra with SdiPBI-S, and the low HOMO energy are encouraging characteristics for PDBT-T1 to be paired with SdiPBI-S as the active layer. Accordingly, the champion PDBT-T1:SdiPBI-S solar cell shows a high PCE of 7.16% with a high fill factor (FF) of 66.1%, V_{oc} of 0.90 V, and short-circuit current density (J_{sc}) of 11.98 mA/cm^2. To the best of our knowledge, this PCE is the highest value reported in the literature to date for non-fullerene polymer solar cells. The results indicate that SdiPBI-S is a promising non-fullerene acceptor material for

DOI: 10.1021/jacs.5b06414
J. Am. Chem. Soc. 2015, 137, 11156−11162

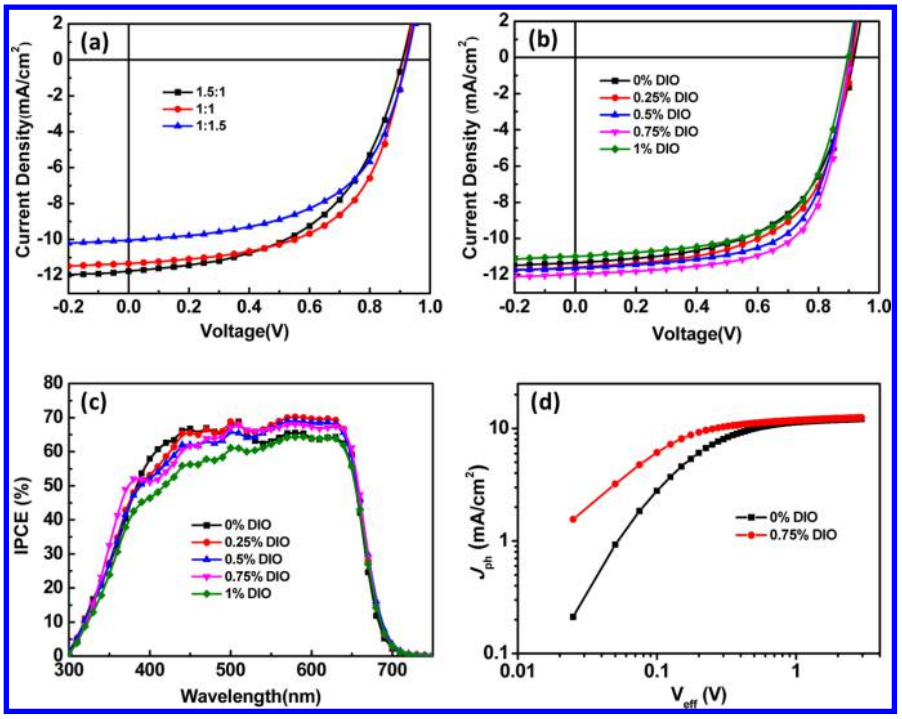

Figure 2. (a) $J-V$ curves of non-fullerene organic solar cells with different PDBT-T1:SdiPBI-S blend ratios. (b) $J-V$ curves of PDBT-T1:SdiPBI-S solar cells with different DIO concentrations and (c) the corresponding IPCE spectra. (d) J_{ph} vs V_{eff} characteristics of PDBT-T1:SdiPBI-S solar cells with and without 0.75% DIO.

application in organic solar cells. Meanwhile, the selection of suitable donor polymers is of crucial importance for realizing high-performance non-fullerene organic solar cells.

RESULTS AND DISCUSSION

Starting from tetrachloro-PBI **1**, 1,12-dichloroperylene bisimide **2** was prepared at 110 °C by the system of CuI and L-proline. The subsequent key intermediate, 1,12-dichloro-6-bromoperylene bisimide **3**, was synthesized in 90.1% yield by bromination of compound **2** under concentrated sulfuric acid. Compound **3** underwent homocoupling to directly afford the singly linked bis(dichloro-PBI) **4**. Finally, SdiPBI-S (**5**) was synthesized through a Stille-type coupling reaction between compound **4** and $Bu_3SnSSnBu_3$ using $Pd(PPh_3)_4$ as the catalyst (Scheme 1). These compounds were fully characterized by ^1H and ^{13}C NMR spectroscopy and high-resolution mass spectrometry (HRMS). SdiPBI-S is highly soluble in common organic solvents such as chloroform and *o*-dichlorobenzene (*o*-DCB) at room temperature. Such optimal solubility is mainly due to both the branched alkyl side chains and the nonplanar molecular scaffold.

To understand the geometric difference between SdiPBI and SdiPBI-S, theoretical calculations were performed using the density functional theory (DFT) at the B3LYP/6-31G(d) level. As shown in Figure 1a,b, the dihedral angle between the two PBI subunits is 67° in SdiPBI and increases to 80° for SdiPBI-S because of its large steric repulsion, suggesting that the introduction of the S bridges into SdiPBI results in a more twisted molecular configuration.

The UV−vis absorption spectra of SdiPBI and SdiPBI-S in dilute chloroform solution (10^{-5} M) are shown in Figure S1. SdiPBI has broad absorptions in the wavelength range of 400−600 nm with a maximum extinction coefficient of 7.7×10^4 M^{-1} cm^{-1} at 523 nm. In contrast, blue-shifted and narrowed multiple absorption peaks throughout the 400−550 nm range were observed for SdiPBI-S, with a dominant peak at 504 nm and $\varepsilon_{max} = 1.4 \times 10^5$ M^{-1} cm^{-1}. Compared to SdiPBI-S in solution, a SdiPBI-S thin film shows similar optical absorption spectra in which the main absorption peaks are maintained at the same positions, indicative of weak aggregation in the solid state. As illustrated in Figure 1d, the main absorption of PDBT-T1 is in the range from 500 to 700 nm, which complements the absorption spectrum of SdiPBI-S. The optimal band gaps (E_g^{opt}) of SdiPBI and SdiPBI-S estimated from the film absorption edges are 2.07 and 2.20 eV, respectively.

Electrochemical cyclic voltammetry (CV) was used to investigate the energy levels (Figure 1e). The LUMO energies of SdiPBI and SdiPBI-S estimated from their onset reduction potentials are close at −3.92 and −3.85 eV, respectively. The S bridges increase the electron density as well as the steric hindrance of the PBI subunits and thus weaken the π conjugation between the PBI units, leading to a larger band gap in SdiPBI-S than in SdiPBI. The HOMO energy of PDBT-T1 is −5.36 eV. The energy offset between the HOMO of PDBT-T1 (−5.36 eV) and the LUMO of SdiPBI-S (−3.85 eV) is 1.51 eV, and thus, a high V_{oc} is anticipated.

In order to evaluate the photovoltaic properties, organic solar cells were fabricated with a conventional device architecture of ITO/PEDOT:PSS/PDBT-T1:SdiPBI-S/Ca/Al, where ITO is indium tin oxide, PEDOT is poly(3,4-ethylenedioxythiophene), and PSS is poly(styrenesulfonate). Ca/Al was used as the cathode. Initially, PDBT-T1:SdiPBI-S mass blend ratios from 1.5:1 to 1:1.5 were tested. The active layer was deposited by spin-casting from chlorobenzene followed by thermal annealing at 100 °C for 5 min. The current density−voltage ($J-V$) curves of the devices are shown in Figure 2a, and the corresponding incident photon conversion efficiency (IPCE) spectra are

DOI: 10.1021/jacs.5b06414
J. Am. Chem. Soc. 2015, 137, 11156−11162

Table 1. Summary of Device Parameters of PDBT-T1:SdiPBI-S Solar Cells with Different DIO Concentrations under AM1.5G Illumination at 100 mW/cm^2

DIO (%)	V_{oc} (V)	J_{sc} (mA/cm^2)	FF (%)	PCE (%)[a]	PCE_{max} (%)
0	0.92 ± 0.003	11.23 ± 0.16	57.1 ± 0.63	5.85 ± 0.16	6.05
0.25	0.91 ± 0.003	11.35 ± 0.17	60.4 ± 0.34	6.24 ± 0.09	6.35
0.5	0.90 ± 0.002	11.47 ± 0.17	64.7 ± 0.16	6.71 ± 0.12	6.81
0.75	0.90 ± 0.003	11.65 ± 0.21	65.5 ± 0.58	6.90 ± 0.15	7.16
1.0	0.90 ± 0.005	10.75 ± 0.18	62.0 ± 0.72	6.03 ± 0.14	6.15

[a]The reported values are average PCEs from five devices.

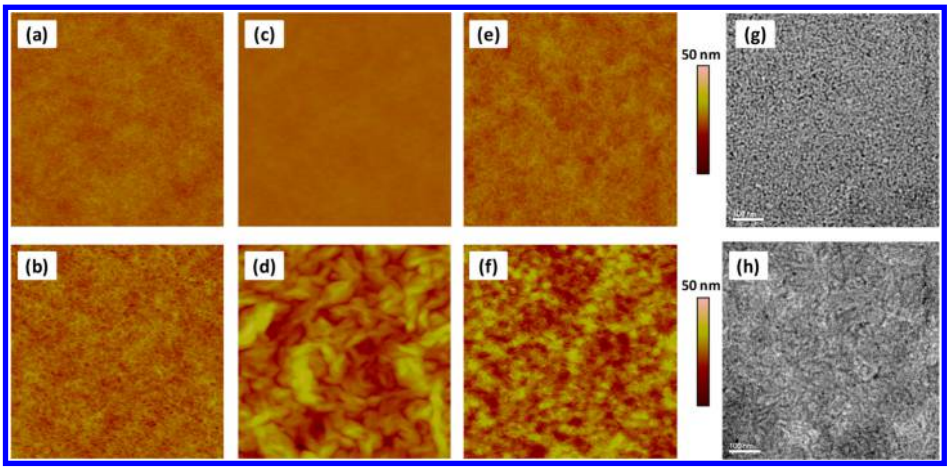

Figure 3. (a–f) AFM topographic images (2 μm × 2 μm) of PDBT-T1 neat films (a) without and (b) with 0.75% DIO, SdiPBI-S neat films (c) without and (d) with 0.75% DIO, and PDBT-T1:SdiPBI-S blend films (e) without and (f) with 0.75% DIO. (g, h) TEM images (scale bar = 100 nm) of PDBT-T1:SdiPBI-S blend films (g) without and (h) with 0.75% DIO.

shown in Figure S3. The device parameters are summarized in Table S1.

Solar cells with a 1:1 blend ratio showed the best performance, with V_{oc} = 0.92 V, J_{sc} = 11.34 mA/cm^2, FF = 58.1%, and PCE = 6.05%. On the basis of 1:1 blend ratio, 1,8-diiodooctane (DIO) was used to further improve the cell performance. The photovoltaic performance of solar cells fabricated with various DIO concentrations is summarized in Table 1, and typical J–V curves of the devices are shown in Figure 2b.

At a DIO concentration of 1%, the solar cells show slightly decreased J_{sc} but increased FF, leading to an efficiency comparable to that of the cell without DIO additive. In contrast, we noted that low DIO concentrations less than 1% could lead to significant improvements in the PCE. At a DIO concentration of 0.25%, the solar cells yielded a high PCE of 6.35% due to the simultaneous improvements in J_{sc} and FF. When the DIO concentration was increased to 0.5%, the PCE went up to 6.81% with V_{oc} = 0.90 V, J_{sc} = 11.64 mA/cm^2, and FF = 64.7%. Further increasing the DIO concentration to 0.75% resulted in a record efficiency of 7.16%. The high PCE is mainly attributed to the increased J_{sc} (11.98 mA/cm^2) and FF (66.1%). To the best of our knowledge, this efficiency is the highest value reported in the literature to date for all types of solution-processed fullerene-free organic solar cells. It should be noted that the FF of non-fullerene organic solar cells has rarely exceeded 65% in previous studies, but our breakthrough results indicate that non-fullerene organic solar cells have enormous potential to approach similar performance as fullerene-based solar cells via careful matching of donor polymers and non-fullerene acceptors and device optimization. Meanwhile, solar cells based on the PDBT-T1/SdiPBI blend were fabricated in parallel for comparison. The J–V curves of these devices are shown in Figure S4. Without the use of DIO additive, the solar cells show a PCE of 5.07% with V_{oc} = 0.89 V, J_{sc} = 9.89 mA/cm^2 and FF = 57.1%. When 0.75% DIO was added into the blend solutions, the efficiency increased to 5.40%, which is still much lower than that of the SdiPBI-S-based solar cells.

The IPCE plots for solar cells with different DIO concentrations are shown in Figure 2c. Solar cells based on the combination of PDBT-T1 and SdiPBI-S yielded broad IPCE spectra from 300 to 800 nm. Except for the cell with 1% DIO, the IPCE values in the wavelength range of 430–650 nm were observed to be higher than 60%; the maximum value was 70%, indicating efficient photon harvesting and charge collection. The J_{sc} value calculated from the IPCE spectrum was 11.55 mA/cm^2, which is in good agreement with the J_{sc} value obtained from the J–V curves (11.98 mA/cm^2) with a 3.7% mismatch.

The bulk charge transport properties of the PDBT-T1:SdiPBI-S blend film was investigated using the space-charge-limited current (SCLC) method.[49] The hole mobility was measured with the device structure ITO/MoO_x/PDBT-T1:SdiPBI-S/MoO_x/Al, and the electron mobility was measured with the device structure ITO/Al/PDBT-T1:SdiPBI-S/Al (Figure S5). The hole mobility was calculated to be μ_h = 1.2 × 10^{-3} cm^2 V^{-1} s^{-1}, and the electron mobility is μ_e = 2.8 × 10^{-3} cm^2 V^{-1} s^{-1}, corresponding to nearly balanced charge transport (μ_e/μ_h = 2.3). Carrier mobilities of PDBT-T1 and SdiPBI-S neat films were also measured (Figure S6). The hole mobility of PDBT-T1 is 8.5 × 10^{-3} cm^2 V^{-1} s^{-1}, and the electron mobility of SdiPBI-S is 3.2 × 10^{-3} cm^2 V^{-1} s^{-1}. The high carrier mobilities and balanced carrier transport in the

DOI: 10.1021/jacs.5b06414
J. Am. Chem. Soc. 2015, 137, 11156–11162

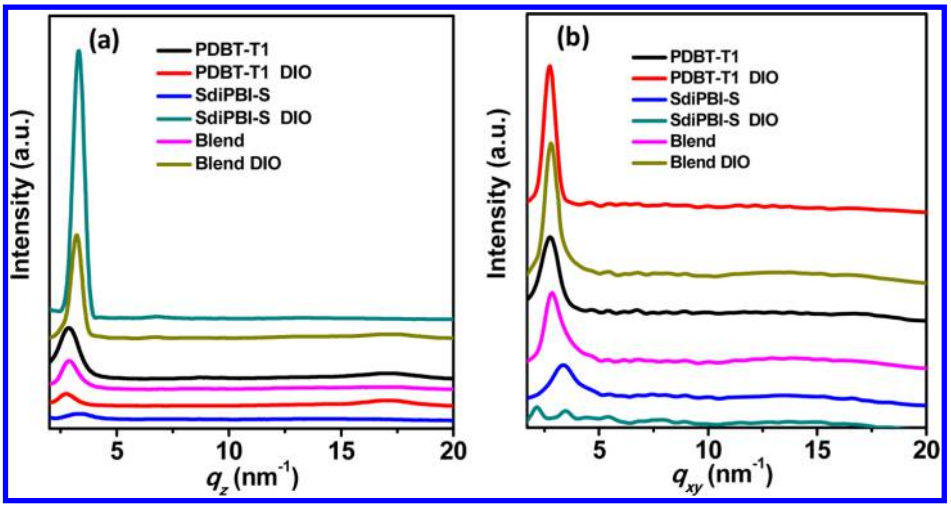

Figure 4. (a) Out-of-plane and (b) in-plane 2D GIWAXS patterns of neat PDBT-T1 and SdiPBI-S films and PDBT-T1:SdiPBI-S blend films with and without 0.75% DIO.

active layer may explain the high PCEs achieved in PDBT-T1:SdiPBI-S solar cells.

The photocurrent density (J_{ph}) as a function of the effective voltage (V_{eff}) of the solar cells was measured to probe the process of excition generation, exciton dissociation, and carrier collection efficiency. J_{ph} is defined as $J_L - J_D$, where J_L and J_D are the current densities under illumination and in the dark, respectively. V_{eff} is defined as $V_0 - V$, where V_0 is the voltage at which J_{ph} is zero and V is the applied voltage.[50] As shown in Figure 2d, at a large reverse voltage (i.e., $V_{eff} \geq 2$ V), J_{ph} reaches saturation (J_{sat}), suggesting that all of the photogenerated excitons are dissociated into free carriers and collected by the electrodes. Thus, the exciton dissociation and charge collection efficiency can be estimated using the J_{ph}/J_{sat} ratio. A high J_{ph}/J_{sat} value of 96.1% was achieved for SdiPBI-S-based solar cells with 0.75% DIO, which is slightly higher than that of solar cells without DIO (95.3%), indicating a higher photogenerated exciton dissociation and charge collection efficiency in DIO-processed solar cells. Under the maximal power output conditions, the J_{ph}/J_{sat} values in PDBT-T1:SdiPBI-S solar cells with and without 0.75% DIO are still as high as 78.5% and 70.5%, respectively, indicative of efficient exciton dissociation at the interface of the PDBT-T1:SdiPBI-S active layer.

The morphologies of PDBT-T1:SdiPBI-S blend films processed under different conditions were studied using atomic force microscopy (AFM). As displayed in Figure 3e, without the use of DIO additive, the surfaces of PDBT-T1:SdiPBI-S blend film are fairly smooth and uniform and show fibrous features with a root-mean-square (RMS) roughness of 1.46 nm. The fibrous structure should be assigned to PDBT-T1, as this feature was also present in its neat film and was not seen in the neat SdiPBI-S film. Dramatic changes in morphology were observed upon addition of DIO solvent additive, as shown in Figure S7. When the DIO concentration was increased from 0.25% to 1%, the fibrous features in the blend films remain unchanged, but with increased aggregate domains, which can also be seen from the corresponding transmission electron microscopy (TEM) images and AFM phase images (Figure 3g,h and Figure S7). In order to determine whether the aggregates mainly arise from the donor or the acceptor, the surface morphologies of PDBT-T1 and SdiPBI-S neat films and the films with 0.75% DIO were also measured. In terms of PDBT-T1, DIO did not induce obvious aggregations, and the films still retained fibrous features. However, large bulky aggregates were observed in SdiPBI-S films, suggesting that SdiPBI-S contributed to the aggregates in the DIO-processed blend films rather than PDBT-T1. The boiling point of DIO is higher than that of the chlorobenzene host solvent, which would allow sufficient time for SdiPBI-S to aggregate, leading to favorable phase separation.

The crystallinity and molecular orientation in both neat and blend films were investigated by grazing-incidence wide-angle X-ray scattering (GIWAXS) measurements.[51] The out-of-plane and in-plane two-dimensional (2D) GIWAXS patterns of neat PDBT-T1 and SdiPBI-S films and PDBT-T1:SdiPBI-S blend films are shown in Figure 4. The neat PDBT-T1 film shows Bragg reflections at $q_z \approx 2.89$ and 17.13 nm^{-1}, which result from the formation of a lamellar structure ($d \approx 21.7$ Å) and $\pi-\pi$ stacking ($d \approx 3.67$ Å), indicating the coexistence of edge-on and face-on orientations. The decreased lamellar diffraction peak and the increased $\pi-\pi$ stacking peak in the out-of-plane direction for the PDBT-T1 film processed with DIO mean that the DIO increased the face-on preference of PDBT-T1 molecules. Compared with the neat SdiPBI-S film, the significantly increased lamellar diffraction peak centered at $q_z \approx 3.29$ nm^{-1} ($d = 19.1$ Å) and the observation of the second-order peaks at 6.72 nm^{-1} suggest the presence of larger crystalline domains in DIO-processed SdiPBI-S films, which agrees well with the AFM height images (Figure 3c,d). The absence of a $\pi-\pi$ stacking peak for SdiPBI-S films with and without DIO indicates a twisted molecular configuration that prevents $\pi-\pi$ stacking of the PBI cores. The PDBT-T1:SdiPBI-S blend film shows packing motifs similar to those for the neat PDBT-T1 film: the lamellar diffraction peak at $q_z \approx 2.89$ nm^{-1} and the $\pi-\pi$ stacking peak at $q_z \approx 17.13$ nm^{-1}. After incorporation of DIO into the blend film, a stronger lamellar diffraction peak at $q_z \approx 3.29$ nm^{-1}, which arises from SdiPBI-S, and an increased $\pi-\pi$ stacking peak in the out-of-plane direction were observed, indicating that a preferred out-of-plane orientation of PDBT-T1 molecules and larger SdiPBI-S aggregate domains formed in the blend films. The results also prove that the large aggregations observed in the AFM height images are attributed to the SdiPBI-S acceptor.

DOI: 10.1021/jacs.5b06414
J. Am. Chem. Soc. 2015, 137, 11156−11162

CONCLUSION

A novel twisted PBI dimer acceptor, SdiPBI-S, was synthesized and applied in BHJ organic solar cells. The introduction of S bridges into the SdiPBI compound resulted in a more twisted molecular configuration and a higher LUMO energy. The two PBI subunits in SdiPBI-S are almost perpendicular to each other, with a dihedral angle of 80°. SdiPBI-S shows a broad absorption in the visible region, which complements well the absorption of the PDBT-T1 donor. Conventional BHJ devices based on a combination of PDBT-T1 and SdiPBI-S processed with 0.75% DIO give the record PCE of 7.16% with an impressive FF of 66.1% and high V_{oc} of 0.90 V. The DIO was found to increase the aggregation of the SdiPBI-S acceptor, leading to favorable phase separation and balanced carrier mobilites in the BHJ films. The excellent photovoltaic performance demonstrates that fine-tuning of PBI-based materials is a promising way to improve the PCEs of non-fullerene BHJ organic solar cells. Moreover, with careful selection of donor materials, non-fullerene organic solar cells can have enormous potential to approach performance similar to that of fullerene-based organic solar cells.

ASSOCIATED CONTENT

Supporting Information

The Supporting Information is available free of charge on the ACS Publications website at DOI: 10.1021/jacs.5b06414.

Experimental details, synthesis, device fabrication and charaterization, UV absorption spectra, and theoretical calculations (PDF)

AUTHOR INFORMATION

Corresponding Authors

*huolijun@buaa.edu.cn
*sunym@buaa.edu.cn
*wangzhaohui@iccas.ac.cn

Author Contributions

⊥D.S. and D.M. contributed equally.

Notes

The authors declare no competing financial interest.

ACKNOWLEDGMENTS

This work was financially supported by the National Natural Science Foundation of China (NSFC) (21225209, 91427303, 21190032, 51473009, and 51273203), the International Science & Technology Cooperation Program of China (2014DFA52820), the 973 Program (2011CB932301, 2012CB932903, and 2014CB643502), NSFC−DFG Joint Project TRR61, and the Chinese Academy of Sciences (XDB12010100). The authors gratefully acknowledge Prof. Z. Wei for the assistance with GIWAXS measurements and Prof. Y. Liu for the help with AFM measurements.

REFERENCES

(1) Sariciftci, N. S.; Smilowitz, L.; Heeger, A. J.; Wudl, F. *Science* **1992**, *258*, 1474−1476.
(2) Heeger, A. J. *Adv. Mater.* **2014**, *26*, 10−28.
(3) Li, G.; Zhu, R.; Yang, Y. *Nat. Photonics* **2012**, *6*, 153−161.
(4) Li, Y. F. *Acc. Chem. Res.* **2012**, *45*, 723−733.
(5) Brabec, C. J.; Gowrisanker, S.; Halls, J. J. M.; Laird, D.; Jia, S. J.; Williams, S. P. *Adv. Mater.* **2010**, *22*, 3839−3856.
(6) Son, H. J.; Carsten, B.; Jung, I. H.; Yu, L. P. *Energy Environ. Sci.* **2012**, *5*, 8158−8170.
(7) Thompson, B. C.; Frechet, J. M. *Angew. Chem., Int. Ed.* **2008**, *47*, 58−77.
(8) Huang, Y.; Kramer, E. J.; Heeger, A. J.; Bazan, G. C. *Chem. Rev.* **2014**, *114*, 7006−7043.
(9) Jiang, W.; Li, Y.; Wang, Z. *Acc. Chem. Res.* **2014**, *47*, 3135−3147.
(10) Ball, M.; Zhong, Y.; Wu, Y.; Schenck, C.; Ng, F.; Steigerwald, M.; Xiao, S.; Nuckolls, C. *Acc. Chem. Res.* **2015**, *48*, 267−276.
(11) Guo, X.; Facchetti, A.; Marks, T. J. *Chem. Rev.* **2014**, *114*, 8943−9021.
(12) Lin, Y.; Li, Y.; Zhan, X. *Chem. Soc. Rev.* **2012**, *41*, 4245−4272.
(13) Li, H.; Hwang, Y. J.; Courtright, B. A. E.; Eberle, F. N.; Subramaniyan, S.; Jenekhe, S. A. *Adv. Mater.* **2015**, *27*, 3266.
(14) Zhong, Y.; Trinh, M. T.; Chen, R.; Wang, W.; Khlyabich, P. P.; Kumar, B.; Xu, Q.; Nam, C. Y.; Sfeir, M. Y.; Black, C.; Steigerwald, M. L.; Loo, Y. L.; Xiao, S.; Ng, F.; Zhu, X. Y.; Nuckolls, C. *J. Am. Chem. Soc.* **2014**, *136*, 15215−15221.
(15) Zhao, J.; Li, Y.; Lin, H.; Liu, Y.; Jiang, K.; Mu, C.; Ma, T.; Lai, J. Y. L.; Hu, H.; Yu, D.; Yan, H. *Energy Environ. Sci.* **2015**, *8*, 520−525.
(16) Lin, Y.; Wang, J.; Zhang, Z. G.; Bai, H.; Li, Y.; Zhu, D.; Zhan, X. *Adv. Mater.* **2015**, *27*, 1170−1174.
(17) Wen, Y.; Liu, Y. *Adv. Mater.* **2010**, *22*, 1331−1345.
(18) Würthner, F. *Chem. Commun.* **2004**, 1564−1579.
(19) Chen, Z.; Lohr, A.; Saha-Möller, C. R.; Würthner, F. *Chem. Soc. Rev.* **2009**, *38*, 564−584.
(20) Li, C.; Wonneberger, H. *Adv. Mater.* **2012**, *24*, 613−636.
(21) Schmidt, R.; Oh, J. H.; Sun, Y.-S.; Deppisch, M.; Krause, A.-M.; Radacki, K.; Braunschweig, H.; Könemann, M.; Erk, P.; Bao, Z.; Würthner, F. *J. Am. Chem. Soc.* **2009**, *131*, 6215−6228.
(22) Dittmer, J. J.; Marseglia, E. A.; Friend, R. H. *Adv. Mater.* **2000**, *12*, 1270−1274.
(23) Li, M.; Wang, L.; Liu, J.; Zhou, K.; Yu, X.; Xing, R.; Geng, Y.; Han, Y. *Phys. Chem. Chem. Phys.* **2014**, *16*, 4528−4537.
(24) Howard, I. A.; Laquai, F.; Keivanidis, P. E.; Friend, R. H.; Greenham, N. C. *J. Phys. Chem. C* **2009**, *113*, 21225−21232.
(25) Kamm, V.; Battagliarin, G.; Howard, I. A.; Pisula, W.; Mavrinskiy, A.; Li, C.; Müllen, K.; Laquai, F. *Adv. Energy Mater.* **2011**, *1*, 297−302.
(26) Shivanna, R.; Shoaee, S.; Dimitrov, S.; Kandappa, S. K.; Rajaram, S.; Durrant, J. R.; Narayan, K. S. *Energy Environ. Sci.* **2014**, *7*, 435−441.
(27) Jiang, W.; Ye, L.; Li, X.; Xiao, C.; Tan, F.; Zhao, W.; Hou, J.; Wang, Z. *Chem. Commun.* **2014**, *50*, 1024−1026.
(28) Ye, L.; Jiang, W.; Zhao, W.; Zhang, S.; Qian, D.; Wang, Z.; Hou, J. *Small* **2014**, *10*, 4658−4663.
(29) Ye, L.; Jiang, W.; Zhao, W.; Zhang, S.; Cui, Y.; Wang, Z.; Hou, J. *Org. Electron.* **2015**, *17*, 295−303.
(30) Zang, Y.; Li, C. Z.; Chueh, C. C.; Williams, S. T.; Jiang, W.; Wang, Z. H.; Yu, J. S.; Jen, A. K. Y. *Adv. Mater.* **2014**, *26*, 5708−5714.
(31) Zhang, X.; Lu, Z.; Ye, L.; Zhan, C.; Hou, J.; Zhang, S.; Jiang, B.; Zhao, Y.; Huang, J.; Zhang, S.; Liu, Y.; Shi, Q.; Liu, Y.; Yao, J. *Adv. Mater.* **2013**, *25*, 5791−5797.
(32) Lin, Y.; Wang, J.; Dai, S.; Li, Y.; Zhu, D.; Zhan, X. *Adv. Energy Mater.* **2014**, *4*, 1400420.
(33) Jiang, B.; Zhang, X.; Zhan, C.; Lu, Z.; Huang, J.; Ding, X.; He, S.; Yao, J. *Polym. Chem.* **2013**, *4*, 4631−4638.
(34) Du, Y.; Jiang, L.; Zhou, J.; Qi, G.; Li, X.; Yang, Y. *Org. Lett.* **2012**, *14*, 3052−3055.
(35) Sharenko, A.; Proctor, C. M.; van der Poll, T. S.; Henson, Z. B.; Nguyen, T. Q.; Bazan, G. C. *Adv. Mater.* **2013**, *25*, 4403−4406.
(36) Yan, Q.; Zhou, Y.; Zheng, Y.-Q.; Pei, J.; Zhao, D. *Chem. Sci.* **2013**, *4*, 4389−4394.
(37) Zhou, Y.; Kurosawa, T.; Ma, W.; Guo, Y.; Fang, L.; Vandewal, K.; Diao, Y.; Wang, C.; Yan, Q.; Reinspach, J.; Mei, J.; Appleton, A. L.; Koleilat, G. I.; Gao, Y.; Mannsfeld, S. C. B.; Salleo, A.; Ade, H.; Zhao, D.; Bao, Z. *Adv. Mater.* **2014**, *26*, 3767−3772.
(38) Cai, Y.; Huo, L.; Sun, X.; Wei, D.; Tang, M.; Sun, Y. *Adv. Energy Mater.* **2015**, *5*, 1500032.
(39) Hwang, Y. J.; Earmme, T.; Courtright, B. A. E.; Eberle, F. N.; Jenekhe, S. A. *J. Am. Chem. Soc.* **2015**, *137*, 4424−4434.
(40) Jiang, W.; Li, Y.; Wang, Z. *Chem. Soc. Rev.* **2013**, *42*, 6113−6127.

DOI: 10.1021/jacs.5b06414
J. Am. Chem. Soc. 2015, 137, 11156−11162

(41) Sun, Y.; Tan, L.; Jiang, S.; Qian, H.; Wang, Z.; Yan, D.; Di, C.; Wang, Y.; Wu, W.; Yu, G.; Yan, S.; Wang, C.; Hu, W.; Liu, Y.; Zhu, D. *J. Am. Chem. Soc.* **2007**, *129*, 1882−1883.
(42) Qian, H.; Liu, C.; Wang, Z.; Zhu, D. *Chem. Commun.* **2006**, 4587−4589.
(43) Jiang, W.; Qian, H.; Li, Y.; Wang, Z. *J. Org. Chem.* **2008**, *73*, 7369−7372.
(44) Li, Y.; Gao, J.; Di Motta, S.; Negri, F.; Wang, Z. *J. Am. Chem. Soc.* **2010**, *132*, 4208−4213.
(45) Jiang, W.; Zhou, Y.; Geng, H.; Jiang, S.; Yan, S.; Hu, W.; Wang, Z.; Shuai, Z.; Pei, J. *J. Am. Chem. Soc.* **2011**, *133*, 1−3.
(46) Hartnett, P. E.; Timalsina, A.; Matte, H. S. S. R.; Zhou, N.; Guo, X.; Zhao, W.; Facchetti, A.; Chang, R. P.; Hersam, M. C.; Wasielewski, M. R.; Marks, T. J. *J. Am. Chem. Soc.* **2014**, *136*, 16345−16356.
(47) Qian, H.; Yue, W.; Zhen, Y.; Di Motta, S.; Di Donato, E.; Negri, F.; Qu, J.; Xu, W.; Zhu, D.; Wang, Z. *J. Org. Chem.* **2009**, *74*, 6275−6282.
(48) Huo, L.; Liu, T.; Sun, X.; Cai, Y.; Heeger, A. J.; Sun, Y. *Adv. Mater.* **2015**, *27*, 2938−2944.
(49) Malliaras, G. G.; Salem, J. R.; Brock, P. J.; Scott, C. *Phys. Rev. B: Condens. Matter Mater. Phys.* **1998**, *58*, R13411.
(50) Blom, P. W. M.; Mihailetchi, V. D.; Koster, L. J. A.; Markov, D. E. *Adv. Mater.* **2007**, *19*, 1551−1566.
(51) Müller-Buschbaum, P. *Adv. Mater.* **2014**, *26*, 7692−7709.

DOI: 10.1021/jacs.5b06414
J. Am. Chem. Soc. 2015, 137, 11156−11162